24th ABCM International Congress of Mechanical Engineering
December 3-8, 2017, Curitiba, PR, Brazil

COBEM-2017-1194

DETERMINATION OF THE HEAT TRANSFER RATE AND FRICTION COEFFICIENT IN CROSS-FLOW FORCED CONVECTION

Leonardo Cavalheiro Martinez
Fernanda Perazzolo Disconzi
José Viriato Coelho Vargas

Post-Graduate Program in Mechanical Engineering (PGMec)
Self-Sustainable Energy Research and Development Center (NPDEAS)
Federal University of Paraná (UFPR) – Av. Cel. Francisco Heráclito dos Santos – 81.530-900 – Curitiba – PR – Brazil

leonardo.cmartinez@live.com
fernandadisconzi@gmail.com
vargasjvcv@gmail.com

Abstract. *This study presents the determination of the heat transfer rate and friction coefficient in the two-dimensional cross-flow around circular tubes of a heat exchanger. For this, the governing equations and the boundary conditions of the mathematical model, based on the formulation of the Finite Element Method (FEM) for heat transfer, it had been solved through the FEAP (Finite Element Analysis Program) program. In this way, it was possible to obtain the numerical results of heat transfer rate per unit length of the tubes and the average friction coefficient of the flow. It was assumed laminar, incompressible and steady-state flow of the air between the tubes. The air properties were maintained constant during simulation based on the film temperature. For the computational domain was used structured mesh with two-dimensional and quadrilateral elements. The obtained numerical solution behavior was as expected. The numerical result of the heat transfer rate per unit length and the average friction coefficient, respectively, were 293.64 Wm^{-1} and 0.1045, agreeing with the result obtained through of an empirical correlation, presenting a deviation of 11.2%. Thus, it can be stated that FEAP is a suitable computational tool for the simulation of cross-flows that involves the convective heat transfer around tubes.*

Key-Words: *Cross-Flow, Finite Element Method, Heat Transfer Rate, Friction Coefficient.*

NOMENCLATURE

x	Plane Direction	[-]	h	Tubes Assembly Width	m
y	Plane Direction	[-]	H	Dimensionaless Length	[-]
z	Plane Direction	[-]	W	Tubes Assembly Height	m
u	Velocity in “x” Direction	ms^{-1}	A	Area	m^2
v	Velocity in “x” Direction	ms^{-1}	k_1	Flow Inlet Length	m
U	Dimensionaless Velocity in “x”	[-]	p	Flow Outlet Length	m
V	Dimensionaless Velocity in “y”	[-]	N_t	Total Number of Tubes	[-]
s	Horizontal Space between Tubes	m	N_{ce}	Elementary Number Channels	[-]
S	Dimensionaless Horizontal Space	[-]	k	Air Thermal Conductivity	$Wm^{-1}K^{-1}$
b	Vertical Space between Tubes	m	ϑ	Kinematic Viscosity	m^2s^{-1}
B	Dimensionaless Vertical Space	[-]	β	Volumetric Expansion Coefficient	$°C^{-1}$
l	Length – Flow Direction	m	c_p	Specific Heat at Constant Pressure	$Wkg^{-1}K^{-1}$
L	Dimensionaless Length	[-]	μ	Dynamic Viscosity	Pa s
D	Diameter of Tubes	m	ρ	Density	$kg\ m^{-3}$

γ	Penalty Parameter	[-]	$C_{f,n}$	Numerical Friction Coefficient	[-]
P	Pressure	Pa	$C_{f,e}$	Empirical Friction Coefficient	[-]
Pr	Prandtl Number	[-]	τ_w	Shear Stress at Wall	Pa
Nu	Nusselt Number	[-]	j_c	Colburn Factor	[-]
Re	Reynolds Number	[-]	$C(\tilde{U})$	Capacity Matrix	[-]
T_w	Wall Temperature of Tubes	°C	$\tilde{U}$	Solution Vector	[-]
T_f	Film Temperature of Air	°C	K	Stiffness Matrix	[-]
T_∞	Inlet Air Temperature	°C	$\hat{K}$	Penalty Matrix	[-]
T_{out}	Outlet Air Temperature	°C	F	Force Vector	[-]
θ_{out}	Dimensionaless Outlet Air Temp.	[-]	2D		Two-Dimensional
Q	Heat Transfer Rate/W	Wm^{-1}	TC		Heat Exchanger
$\dot{m}_t$	Total Mass Flow	$kg\ s^{-1}$	FEAP		Finite Element Analysis Program
$\tilde{q}$	Dimensionaless Heat Transfer	[-]	MEF		Finite Element Method

1. INTRODUCTION

Heat exchangers are equipment designed to carry out the process of thermal exchange between two systems, e.g. hot fluid and cold fluid, according to the Laws of Thermodynamics and, therefore, to provide the reutilization of thermal energy present in hot fluids (Bejan, 2000). In this way, by conserving energy, heat exchangers become important tools for preserving the environment and maintaining the energy matrix. This equipment is widely used in several engineering sectors such as heaters, refrigerators, air conditioners, heat recuperators, power plants, chemical plants, petrochemical plants, petroleum refineries, natural gas processing and waste waters.

There are few heat exchangers where fluids are in direct contact with each other. In most of them, heat transfer takes place through a separation surface in which heat flows from one fluid to the other (Shah and Sekulic, 2003). In addition, among the various types of exchanger, the shell-and-tube heat exchanger stands out due to its numerous applications and, therefore, is perhaps the most widely used exchanger in the industry.

According to the scientific literature, there are several studies, both experimental and numerical, developed with the purpose of optimizing the heat transfer, investigating the best configuration and geometry of the pipe arrangement. One of the first works found on the subject is that of Shepherd (1956) who analyzed circular tubes with a row and heat exchangers with fins determining the global coefficient of heat transfer as a function of the Reynolds number, assuming isothermal fins.

In addition, Brauer (1964) presented a research with experimental results comparing elliptical and circular tube arrangements for heat transfer and pressure drop, noted that the geometry of the elliptical tube has a better aerodynamic configuration than that of the circular tube. For a turbulent flow, the elliptical tubes had a heat transfer rate 15% highest and pressure drop 18% lowest than in the circular tubes.

Saboya and Sparrow (1976) analyzed three-row circular tube heat exchangers. The results showed low coefficients of mass transfer behind the tubes, when compared with the average of the arrangements. Jang *et al.* (1998) studied experimentally and numerically the flow and the heat transfer in heat exchangers of finned circular tubes of 4 rows with alternating arrangement. Two types of finned tube configurations were investigated under dry and wet conditions for values different from the front velocity of the inlet ranging from 1 to 6 m/s. Wang et al. (2000) proposed a correlation to determine the heat transfer and the friction in finned heat exchangers of fins plane geometry. A total of 74 samples were used to develop the correlations. The proposed heat transfer correlation can describe 88.6% of the samples, while the correlation of friction can correlate 85.1% of the samples.

Taking these studies into account, the present work intends to evaluate the heat transfer rate and the friction coefficient in the flow of a heat exchanger in two dimensions (2-D) with a tubes arrangement of cross-section and cross-flow, i.e. the heated fluid flows into the tubes and the refrigerant flows through the outer side of the tubes, perpendicular to the heated fluid. The global configuration of the heat exchanger and the geometry values of the studied arrangement in this work were not based on an existing configuration due to the wide variety of dimensions found in the scientific literature.

2. PHYSICAL PROBLEM

The physical problem is a typical configuration of a cross flow heat exchanger with two rows of alternating distribution tubes as shown in Fig. 1. The module consists of a set of unfinished circular tubes, the interior of which flows a heated fluid, while externally flows, transversely, the refrigerant fluid. The tubes are mounted in a volume (LHW), where L represents the length oriented in the flow direction, H corresponds to the width of the arrangement and W denotes the height of the arrangement, perpendicular to the flow direction. The tubes are identical, where each circular tube has the characteristic size of the diameter, D. The movement of the fluid in the "z" direction can be disregarded, thus being a two-dimensional flow (x-y plane). The velocity components, "u" and "v", are aligned with the "x" and "y" axes, respectively. By setting the D/l ratio, one can calculate the optimal spacing between the tubes, "s", through the relationship developed by Stanescu et al. (1996) in Eq. (1). The corresponding values of the arrangement dimensions are shown in Table 1.

$$\frac{s}{D} \cong 2.2\mathrm{Pr}^{-0,13}\left(\frac{D}{l}\right)^{-2/5}\mathrm{Re}_D{}^{-3/10} \tag{1}$$

Table 1. Arrangement Dimensions.

Dimension	**Value (mm)**
D	15
l	260
H	75
s	Eq. (1)
b	55

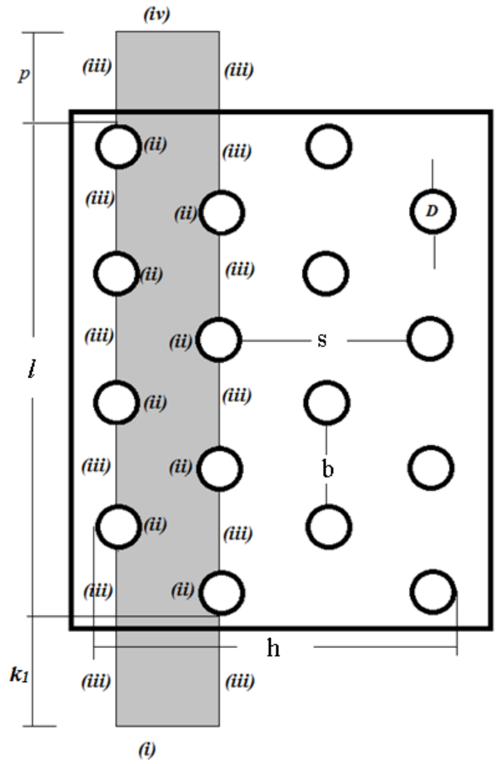

Figure 1. Top View of the Heat Exchanger with highlight for the Simulation Cell.
Source: The Authors (2017).

The external surfaces of the tubes can be considered isothermal, whose temperature is maintained constant in T_w = 100°C. The refrigerant fluid flowing between the exchanger tubes was treated as air, i.e. an ideal gas, the properties of which were determined based on the film temperature ($T_f = (T_w + T_\infty)/2$), equal to 60°C, at atmospheric pressure (1 atm or 101.325 kPa) and kept constant during the simulation. The values of the physical properties of air are shown in Table 2.

Table 2. Atmospheric Air Properties.

Property	**Value (T_f = 60°C, P = 1 atm)**
ρ	1.060 x 10^{-9} [kg/mm^3]
μ	2.000 x 10^{-8} [kg/mm.s]

c_p	1.006 x 10^9 [mm²/s²K]
β	3.003 x 10^{-3} [1/K]
k	28.000 [mm/s³K]
Pr	0.7 [-]

3. MATHEMATICAL MODELLING

Taking into account the physical problem of the heat exchanger and assuming the simplifications of Newtonian fluid, incompressible flow, laminar and two-dimensional flow, permanent regime, constant fluid properties and negligible heat generation and viscous dissipation, the governing equations for the present problem are summarized as follow (Bejan, 1995):

(i) Mass Conservation:

$$\frac{\partial u}{\partial x}+\frac{\partial v}{\partial y}=0 \tag{2}$$

(ii) Momentum Conservation, respectively, on “x” and “y” Directions:

$$u\frac{\partial u}{\partial x}+v\frac{\partial u}{\partial y}=-\frac{1}{\rho}\frac{\partial P}{\partial x}+\nu\left(\frac{\partial^2 u}{\partial x^2}+\frac{\partial^2 u}{\partial y^2}\right) \tag{3}$$

$$u\frac{\partial v}{\partial x}+v\frac{\partial v}{\partial y}=-\frac{1}{\rho}\frac{\partial P}{\partial y}+\nu\left(\frac{\partial^2 v}{\partial x^2}+\frac{\partial^2 v}{\partial y^2}\right) \tag{4}$$

(iii) Energy Conservation:

$$\frac{\partial T}{\partial x}+\frac{\partial T}{\partial y}=\alpha\left(\frac{\partial^2 T}{\partial x^2}+\frac{\partial^2 T}{\partial y^2}\right) \tag{5}$$

The simulated area (Simulation Cell) is represented by the shaded area showed in Fig. 1, where it is possible to identify the contours of the problem [(i), (ii), (iii) and (iv)]. In addition, the boundary conditions in the simulated cell are given as:

(i) Input: $T_\infty = 20°C;\ u = 0;\ v = 0.126\ m/s$ (For $Re = 100$)
(ii) Tubes Wall: $T_s = 100°C;\ u = 0;\ v = 0$
(iii) Simetry Condition: $u = 0;\ \partial v/\partial x = \partial T/\partial x = 0$
(iv) Output (Free Boundary): $\partial u/\partial y = \partial v/\partial y = \partial T/\partial y = 0$ (6)

The Reynolds number, which characterizes the laminar or turbulent nature of the flow and based on the characteristic dimension D, is calculated as:

$$Re_D=\frac{vD}{\nu}=\frac{\rho vD}{\mu} \tag{7}$$

where v refers to velocity and ν to the kinematic viscosity of the fluid flowing into the tubes. In order to normalize and dimensionless the Equations (2) to (5), that is, to obtain numerical stability by making the variables of the model approximately unitary, the following sets of dimensionless variables were considered, as shown by Equations (8) to (10).

$$\theta=\frac{T-T_\infty}{T_w-T_\infty} \tag{8}$$

$$S = s/D,\ L = l/D \text{ and } H = h/D \tag{9}$$

$$U = u/U_\infty \text{ and } V = v/U_\infty \tag{10}$$

3.1 Heat Transfer Rate

In order to be possible calculate the amount of heat exchanged between the fluids during the flow (Q), the output information of the simulation cell, such as T_{out}, is taken into account. Such temperature can be obtained from Equation (11).

$$T_{out} = \theta_{out}(T_w - T_\infty) + T_\infty \quad (11)$$

where T_w and T_∞, respectively, correspond to the wall temperature and the temperature of the fluid (air) at the entrance of the simulation cell. Thus, it is possible to calculate Q through Eq. (12).

$$Q_n = \dot{m}_t c_p (T_{out} - T_\infty) \quad (12)$$

where $\dot{m}_t$ represents the mass flow of air flowing between the tubes, calculated by Eq. (13), and c_p denotes the specific heat at constant pressure (Table 2).

$$\dot{m}_t = \rho v A N_{ce} \quad (13)$$

where ρ corresponds to the specific mass of the air, shown in Table 2, v denotes the velocity of the air in flow obtained as a function of Reynolds number and $A = \left(\frac{S+D}{2}\right) W = 0.020W$, W refers to the height dimension of the tube arrangement. In addition, the term N_{ce} corresponds to the number of elementary channels of the simulation cell.

3.2 Dimensionaless Heat Transfer Rate

According to Stanescu et al. (1996), Matos et al. (2001) and Marchi and Hobmeier (2007), it is possible to obtain the dimensionless heat transfer rate or dimensionless heat transfer volumetric density, $\tilde{q}$, through:

$$\tilde{q} = \frac{QD^2}{kHLW(T_w - T_\infty)} \quad (14)$$

where Q is obtained through Eq. (12), D refers to the diameter of the tubes, the term (HLW) denotes the total volume of the heat exchanger and k corresponds to the thermal conductivity of the air (Table 2).

3.3 Nusselt Number

In order to calculate the numerical Nusselt number, according to Incropera, DeWitt and Bergman (2008), must to be used the Eq. (15) which takes into account the amount of heat, Q, the diameter of the tubes, D, the total number of tubes, N_t, the thermal exchange area, A, the temperature variation between the wall and the air, $T_w - T_\infty$, and the air thermal conductivity, k.

$$Nu_n = \frac{QD}{N_t k A (T_w - T_\infty)} \quad (15)$$

According to Zukauskas (1987), an empirical and adequate correlation for the calculation of the Nusselt number for cross-flow is given by Eq. (16).

$$Nu_e = 0.52 Pr^{0,37} Re^{0,5} \quad (16)$$

3.4 Friction Coefficient

The calculation of the average friction factor obtained in the flow between the refrigerant and the tubes (C_f), takes into account its definition, according to Eq. (17).

$$C_{f,n} = \frac{\tau_w|_{y=0}}{\frac{1}{2}\rho v^2} \quad (17)$$

where $\tau_w|_{y=0}$ represents the shear stress in the wall at y = 0, calculated by:

$$\tau_w|_{y=0} = \mu\left[\frac{du}{dy} + \frac{dv}{dx}\right] \tag{18}$$

In addition, Incropera, DeWitt and Bergman (2008) cite an empirical correlation for the calculation of the friction coefficient based on the Colburn factor, j_c, as shown in Eq. (19).

$$C_{f,e} = 2j_c = 2\frac{Nu}{RePr^{1/3}} \tag{19}$$

where Nu refers to the Nusselt number, obtained by Eq. (15) or (16), Re corresponds to the Reynolds number, calculated through Eq. (7), and Pr denotes the Prandtl number, taking into account a constant value of $Pr = 0.7$, as showed in Table 2.

4. NUMERICAL SOLUTION

The governing differential equations are characterized by being partial equations that, in general, have exact solutions difficult to obtain, or even impossible to obtain. Thus, through of a numerical method, the problem can be solved by an approximation form. Through the numerical method, the differential equations are replaced by algebraic equations and the continuous domain is replaced by a discrete domain. The computational domain consists of the unit cell, which has a total length of 440 mm (Figure 1). For this, in the numerical simulations in Fortran®, the length 90 mm was added at the entrance and exit of the arrangement, as represented in Figure 1, respectively, by the dimensions "k_1" and "p".

The numerical solution of Eq. (2) to (5) with the boundary conditions of Eq. (6) was obtained using the Finite Element Method (Zienkiewicz and Taylor, 1989). For the numerical implementation in Fortran®, the Penalty model was used (Hughes, 1979), in which the pressure is eliminated from the Equation of Conservation of the Motion Quantity, Equations (3) and (4), assuming a slight compressibility to Continuity Equation, in Eq. (2). Therefore:

$$\frac{\partial u}{\partial x} + \frac{\partial v}{\partial y} = -\frac{P}{\gamma} \tag{20}$$

where γ is treated as the penalty parameter according to Hughes (1979) where, in this work, $\gamma = 10^6$ was adopted.

The differential equations and boundary conditions (strong form) are transformed into the weak form by the Galerkin Weighted Residues Method (Grandin, 1991). After obtaining the weak form, the equations can be discretized and the "up-wind" discretization scheme, proposed by Hughes (1979), was used in the numerical solution of the problem due to the fact that the Galerkin method does not capture physical aspects in its discrete equations in its convective plot. Thus, the algebraic equations of the problem, in matrix form, for a two-dimensional, steady-state flow are given by Eq. (21):

$$\begin{bmatrix} C(\tilde{U}) & 0 \\ 0 & C(\tilde{U}) \end{bmatrix}\begin{Bmatrix} \tilde{U}_1 \\ \tilde{U}_2 \end{Bmatrix} + \begin{bmatrix} 2K_{11} + K_{22} & K_{21} \\ K_{12} & K_{11} + 2K_{22} \end{bmatrix} + \begin{bmatrix} \hat{K}_{11} & \hat{K}_{12} \\ \hat{K}_{21} & \hat{K}_{22} \end{bmatrix}\begin{Bmatrix} \tilde{U}_1 \\ \tilde{U}_2 \end{Bmatrix} = \begin{Bmatrix} F_1 \\ F_2 \end{Bmatrix} \tag{21}$$

where $\tilde{U}$ is the solution vector composed of $\tilde{U}_1$ e $\tilde{U}_2$; $C(\tilde{U})$ is the capacity matrix containing the advective terms of the momentum equations, which are nonlinear because they depend on the solution $\tilde{U}$; The terms $K_{11}, K_{12}, K_{21}, K_{22}$ are the stiffness matrices of constant coefficients containing the viscous terms of the momentum equations and $\hat{K}_{11}$, $\hat{K}_{12}$, $\hat{K}_{21}$, $\hat{K}_{22}$ are the penalty matrices.

5. RESULTS AND DISCUSSIONS

The cross-flow heat exchanger (HE) was modeled computationally in the FEAP (Finite Element Analysis Program). The Fig. 2 represents the mesh generated by the Authors (2017) for the computational domain, formed by four nodes quadrilateral elements and with emphasis on the HE output region. With the numerical solution of this computational code, it was possible to obtain the dimensionless temperature at the output of the heat exchanger, that is, soon after the thermal exchange that occurs in the tubes and disregarding the output length "p". This is due to the fact that the heat transfer occurs only while there is influence of the air in transverse flow to the tubes, that is, there is significant heat transfer along the length L = 260 mm. Thus, according to the FEAP program, between nodes 3521 and 3536 (Figure 2), $\theta_{out} = 0.684130$. Taking this value into account and using Eq. (6) and (11), the dimensional temperature at the output of the heat exchanger is $T_{out} = 74.73$ °C.

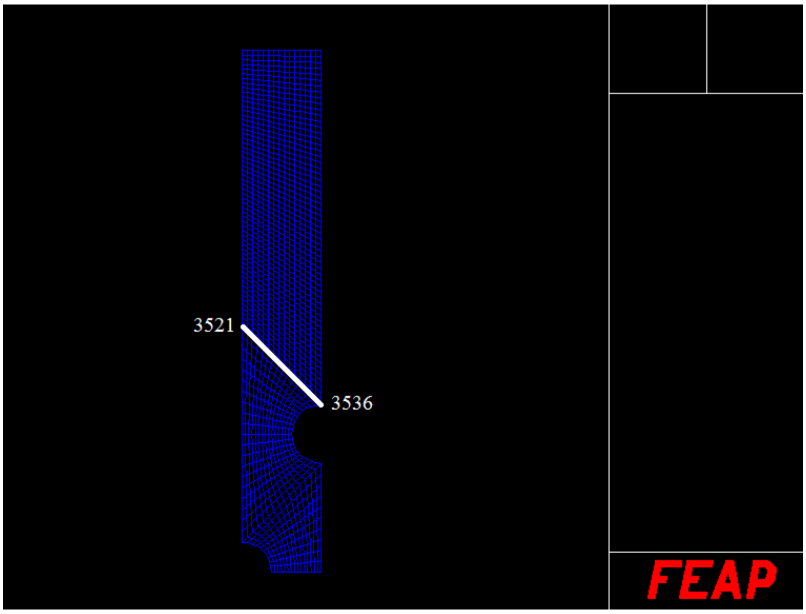

Figure 2. Computational Mesh of the Heat Exchanger with emphasis on the Outflow Region.
Source: The Authors (2017).

For a Reynolds value of $Re = 100$ and using Eq. (7), the air velocity v = 0.126 m / s. Assuming that the number of elementary channels of the simulation cell is $N_{ce} = 2$ and that the specific mass of the air is given in Table 2, the total air mass flow that is flowing through the tubes, $\dot{m}_t$, calculated from Eq. (13), is $\dot{m}_t = 0.0053W$ kg/ s. In order to obtain the heat transfer rate between the fluids circulating inside and outside the heat exchanger tubes as a function of the dimension W, Q/W, it is necessary to use Eq. (12). Thus, you can write the relation $Q_n/W = 293.64$ [W/m], as the numerical result.

With the correlation for Nusselt presented in Eq. (16), it is possible to estimate the value of the convection heat transfer coefficient, h, and, consequently, to determine the value of the heat transfer rate, Q, given by Newton's Cooling Law $[Q_e = hA(T_w - T_\infty)]$ in order to compare with the numerical result. The value calculated by the empirical correlation is Nu = 4.56 and therefore $Q_e/W = 256.72$ [W/m]. Thus, the percentage difference between the numerical value, calculated with the FEAP program, and that obtained through the empirical correlation (Newton's Cooling Law) is approximately 14.4%.

Using the Eq. (17) and (18), it was possible to calculate, numerically, the average friction coefficient, C_f, on the walls of the tubes that compose the heat exchanger. Thereby, a value of $C_{f,n} = 0.1045$ was obtained. For the comparison purpose, it uses Eq. (19) which treats an empirical correlation based on the Colburn factor for the calculation of $C_{f,e}$ and taking into account the Nusselt number (Nu = 5.225), according to Eq. (15). The value calculated by the correlation is $C_{f,e} = 0.1177$ and the percentage difference of the error between the numerical and empirical coefficients is 11.2%.

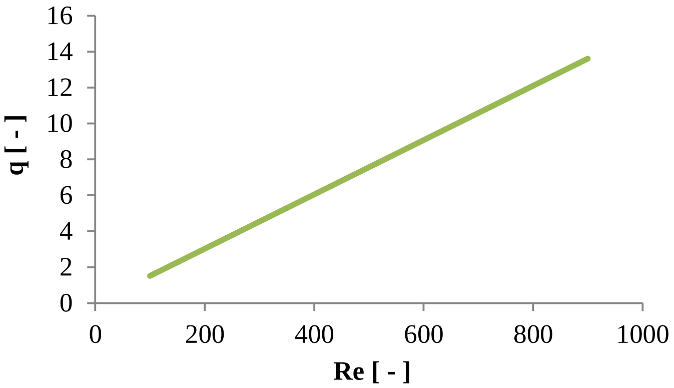

Figure 3. Behavior of $\tilde{q}$ in relation to the Reynolds Number. Source: The Authors (2017).

According to the calculation procedure shown in Eq. (14), the dimensionless heat transfer rate, also called the dimensionless heat transfer volumetric density, for Re = 100, is equivalent to $\tilde{q} = 1.52$. Since this parameter, $\tilde{q}$, is written as a function of the Reynolds number, the Figure 3 shows the graphical behavior of $\tilde{q}$ in relation to the Reynolds variation.

According to Figure 3, the behavior of the dimensionless heat transfer volumetric density, $\tilde{q}$, relative to the Reynolds number is, coincidentally, linear. Such behavior was expected and is due, exclusively, to the fact that all parameters influencing the Reynolds number of Eq. (14), which describes $\tilde{q}$, such as, for example, air flow velocity (v) and dimensional heat transfer rate (Q), are linear.

The Fig. 4, 5 and 6, respectively, represents the flow absolute velocity vectors, the air velocity profile in the "y" direction and the flow temperature field. As can be seen in Fig. 4, as the fluid approaches the tubes, there is a deceleration region of the refrigerant (air) in the front of the same and subsequent acceleration of the flow in the side. Moreover, in both Fig. 4 and Fig. 5, it is possible to note that behind the tubes there is the presence of air recirculation regions, due to the fact that the velocity layer detaches from the tubes wall, by the presence of an adverse pressure gradient, causing the fluid to move in the opposite direction of the direction of the main flow.

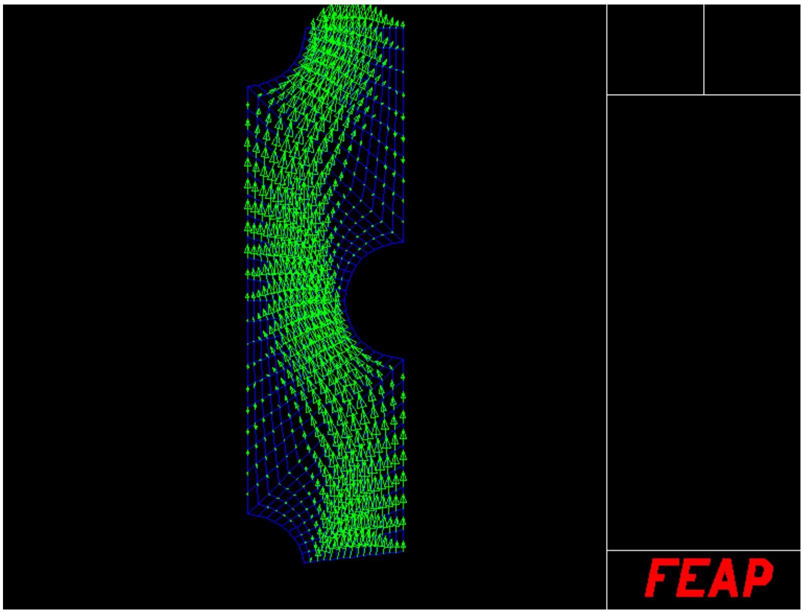

Figure 4. Absolute Velocity Vector.
Source: The Authors (2017).

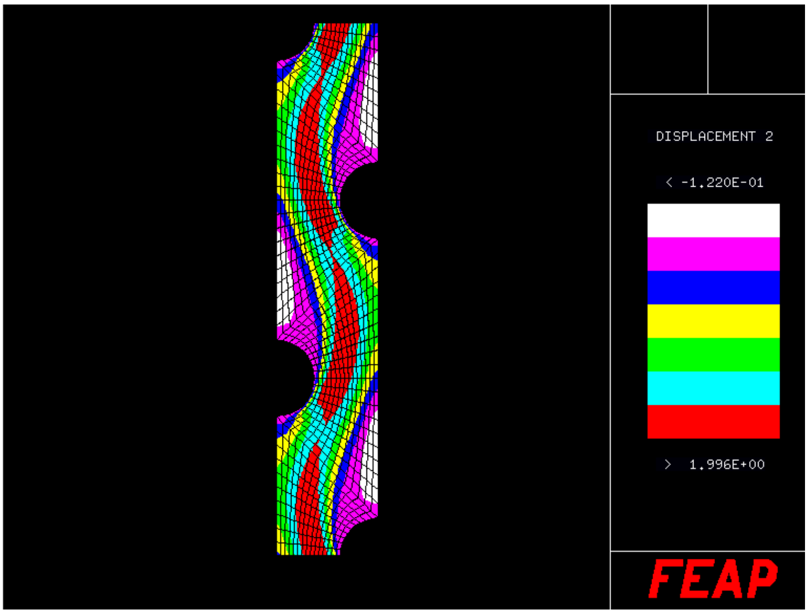

Figure 5. Air Velocity Profile in the "y" Direction.
Source: The Authors (2017).

As can be seen in Figure 6, in regions where fluid is recirculated, the air movement is very small or practically stagnant, causing a heat transfer with predominantly conductive behavior. In addition, due to the recirculation's phenomena, there is a concentration of numerical temperatures in these regions directly due to the fact of a low rate of heat transfer.

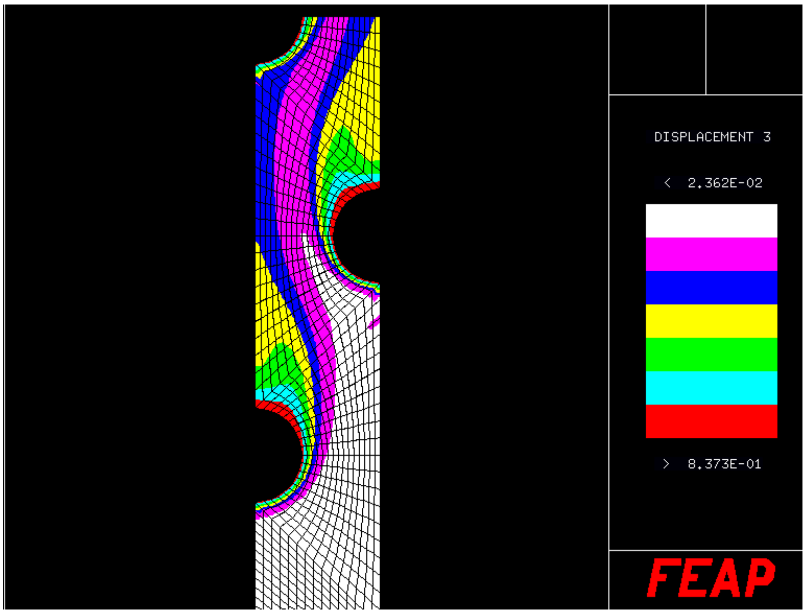

Figure 6. Flow Temperature Distribution (Emphasis shows the Flow Initial Region of the HE)
Source: The Authors (2017).

6. CONCLUSIONS

Through computational simulations in the FEAP program, it was possible to obtain the heat transfer rate per length unit and the average friction coefficient in the cross-flow and two-dimensional flow of a circular tube heat exchanger. The numerical results, obtained by the FEAP program, were presented as expected and, in addition, the heat transfer rate and the friction coefficient agree with the empirical results calculated through Equations (17) and (19), respectively, with a deviation of, approximately, 14.4% and 11.2%. In general, it can be affirmed that the FEAP (Finite Element Analysis Program) is a suitable computational tool for the simulation of flows that involves heat transfer problems.

7. ACKNOWLEDGEMENTS

The authors are grateful for the support received from the National Council for Scientific and Technological Development (CNPq), the Coordination for the Improvement of High Education Personnel (CAPES), the Graduate Program in Mechanical Engineering (PGMec), the Self-Sustainable Energy Research and Development Center (NPDEAS) and the Federal University of Paraná (UFPR).

8. REFERENCES

Bejan, A., 1995. *Convection Heat Transfer*, 2nd Edition, Wiley.

Bejan, A., 2000. *Shape and Structure, from Engineering to Nature*, Cambridge University Press.

Brauer, H. 1964. Compact Heat Exchangers. *Chemical Process Engineering*, p. 451-460.

Grandin, H., 1991. *Fundamentals of the Finite Element Method*, Waveland Press.

Incropera, F.P., De Witt, D.P. and Bergman, T., 2008. *Mass and Heat Transfer Fundamentals*. 6. ed. Rio de Janeiro: LTC, p. 643. *(in Portuguese)*

Jang, J.Y., Lai, J.T., Liu, L.C., 1998. The Thermal-Hydraulic Characteristics of Staggered Circular Finned-Tube Heat Exchangers under Dry and Dehumidifying Conditions. *International Journal of Heat and Mass Transfer*, vol. 41, p. 3321-3337.

Marchi, C.H., Hobmeier, M.A., 2007. Numerical Solution of Staggered Circular Tubes in Two-Dimensional Laminar Forced Convection. *Journal of Brazilian Society Mechanical Sciences and Engineering*. Vol. 29, n. 1, p. 42-48.

Matos, R.S., Vargas, J.V.C., Laursen, T.A., Saboya, F.E.M., 2001. Optimization Study and Heat Transfer Comparison of Staggered Circular and Elliptic Tubes in Forced Convection, *International Journal of Heat and Mass Transfer*, vol. 44, p. 3953-3961.

Saboya, F.E.M. and Sparrow, E.M., 1976. Experiments on a Three-Row Fin and Tube Heat Exchangers. *Journal of Heat Transfer*, vol. 98, p. 520-522.

Shepherd, D.G., 1956. Performance of One-Row Tube Coils with Thin, Plate Fins, Low Velocity Forced Convection. *Heating, Piping and Air Conditioning*, vol. 28, p. 137-144.

Stanescu, G., Fowler, A.J. and Bejan, A., 1996. The Optimal Spacing of Cylinders in Free-Stream Cross-Flow Forced Convection. *International Journal of Heat and Mass Transfer*, vol. 39, p. 311-317.

Wang, C.C., Chi, K.Y. and Chang, C.J., 2000. Heat Transfer and Friction Characteristics of Plain Fin-and-Tube Heat Exchangers, Part II: Correlation. *International Journal of Heat and Mass Transfer*, vol. 43, p. 2693-2700.

Zienkiewicz, O.C. and Taylor, R.L., 1989. *The Finite Element Method*, vol. 1, McGraw-Hill.

Zukauskas, A., 1987. Convective heat transfer in cross flow. *In Handbook of Single-Phase Convective Heat Transfer* (Edited by S. Kakac, R. K. Shah and W. Aung), Chap. 6. Wiley, New York.

9. RESPONSIBILITY NOTICE

The authors are the only responsible for the printed material included in this Paper.